Moon BG, Takaki S, Miyake K, Takatsu K.	The role of IL-5 for mature B-1 cells in homeostatic proliferation, cell survival, and Ig production.	*J Immunol.*	172	6020-6029	2004
Moon BG, Takaki S, Nishizumi H, Yamamoto T, Takatsu K.	Abrogation of autoimmune disease in Lyn-deficient mice by the deletion of IL-5 receptor alpha chain gene.	*Cell Immunol.*	228	110-118	2004
Tamura T, Ariga H, Kinashi T, Uehara S, Kikuchi T, Nakada M, Tokunaga T, Xu W, Kariyone A, Saito T, Kitamura T, Maxwell G, Takaki S, Takatsu K.	The role of antigenic peptide in CD4+ T helper phenotype development in a T cell receptor transgenic model.	*Int Immunol.*	16	1691-1699	2004
Iseki M, Kubo-Akashi C, Kwon SM, Yamaguchi A, Takatsu K, Takaki S.	APS, an adaptor molecule containing PH and SH2 domains, has a negative regulatory role in B cell proliferation.	*Biochem Biophys Res Commun.*	330	1005-1013	2005

Asymmetric Division and Lineage Commitment at the Level of Hematopoietic Stem Cells: Inference from Differentiation in Daughter Cell and Granddaughter Cell Pairs

Hina Takano,[1,2] Hideo Ema,[1] Kazuhiro Sudo,[2] and Hiromitsu Nakauchi[1,2]

[1]*Laboratory of Stem Cell Therapy, Center for Experimental Medicine, Institute of Medical Science, The University of Tokyo, Tokyo 108-8639, Japan*

[2]*Department of Immunology, Institute of Basic Medical Sciences, University of Tsukuba, 305-8575 Tsukuba, Japan*

Abstract

How hematopoietic stem cells (HSCs) commit to a particular lineage is unclear. A high degree of HSC purification enabled us to address this issue at the clonal level. Single-cell transplantation studies revealed that 40% of the $CD34^{-/low}$, c-Kit^+, Sca-1^+, and lineage marker$^-$ ($CD34^-$KSL) cells in adult mouse bone marrow were able, as individual cells, to reconstitute myeloid and B- and T-lymphoid lineages over the long-term. Single-cell culture showed that >40% of $CD34^-$KSL cells could form neutrophil (n)/macrophage (m)/erythroblast (E)/megakaryocyte (M) (nmEM) colonies. Assuming that a substantial portion of long-term repopulating cells can be detected as nmEM cells within this population, we compared differentiation potentials between individual pairs of daughter and granddaughter cells derived in vitro from single nmEM cells. One of the two daughter or granddaughter cells remained an nmEM cell. The other showed a variety of combinations of differentiation potential. In particular, an nmEM cell directly gave rise, after one cell division, to progenitor cells committed to nm, EM, or M lineages. The probability of asymmetric division of nmEM cells depended on the cytokines used. These data strongly suggest that lineage commitment takes place asymmetrically at the level of HSCs under the influence of external factors.

Key words: hematopoiesis • cell differentiation • cell lineage • cell division • cytokines

Introduction

One of the central tasks of stem cell biology is to understand the mechanisms that regulate lineage commitment of stem cells (1–3). Despite the fact that hematopoietic stem cells (HSCs) are the best characterized stem population (4), how they differentiate is poorly understood. Several models have been proposed to explain HSC fate determination. Analyses of in vivo as well as in vitro colony-forming cells (CFCs), particularly CFCs obtained from blast cell colonies, have suggested a stochastic model for HSC behavior (5–13). Consistent with this model, a permissive role for cytokines has also been suggested (12, 14, 15). The classic hematopoietic inductive microenvironment (16) and stem cell competition models (17) have held that extrinsic factors play an instructive role. This idea has been supported by lineage analysis of the progeny of CFCs (18–20). Because no previous paper has verified these working models by directly examining HSCs, whether extrinsic signaling plays any role in HSC lineage commitment remains controversial.

Fate decision in HSCs (self-renewal, differentiation, or apoptosis) takes place through their cell division. Therefore, to study lineage commitment in HSCs, we sought to determine the differentiation potential of the immediate progeny of HSCs at the clonal level. That HSCs are highly enriched in a population of $CD34^{-/low}$, c-Kit^+, Sca-1^+, and lineage marker$^-$ ($CD34^-$KSL) cells among bone marrow cells of the adult mouse has enabled both in vitro and in vivo clonal analyses of HSCs (21, 22). Cytokines such as IL-3 and thrombopoietin (TPO) together with stem cell factor (SCF) directly acted on these cells and induced their division

Address correspondence to Hiromitsu Nakauchi, Laboratory of Stem Cell Therapy, Center for Experimental Medicine, Institute of Medical Science, The University of Tokyo, 4-6-1 Shirokanedai, Minato-ku, 108-8639 Tokyo, Japan. Phone: 81-3-5449-5330; Fax: 81-3-5449-5451; email: nakauchi@ims.u-tokyo.ac.jp

The present address of H. Takano is the Dept. of Hematology, Musashino Red Cross Hospital, 1-26-1 Kyonan, Musashino, 180-8610 Tokyo, Japan.

Abbreviations used in this paper: bl, blastlike; CFC, colony-forming cell; CMP, common myeloid progenitor; E, erythroblast; EPO, erythropoietin; HSC, hematopoietic stem cell; m, macrophage; M, megakaryocyte; n, neutrophil; SA, streptavidin; SCF, stem cell factor; TPO, thrombopoietin.

(22). After CD34$^-$KSL cells underwent one cell division, stem cell activity became undetectable in their progeny except in limited cases, where this activity was maintained in one of the two daughter cells (22, 23). We assumed that lineage commitment could be responsible for loss of stem cell activity in this setting. To verify this hypothesis, we rigorously examined the differentiation potential of paired daughter cells arisen from single CD34$^-$KSL cells in vitro.

Despite a lack of information on lymphoid differentiation potential, in vitro colony assay permits quantitative evaluation of differentiation potential along neutrophil (n), macrophage (m), erythroblast (E), and megakaryocyte (M) lineages at the single-cell level. In this work, using in vitro colony assays, we demonstrated that lineage commitment of multipotent CD34$^-$KSL cells occurs at the initial stage of their cell divisions, and that this lineage commitment is asymmetric. Treatment with certain cytokines increases the chance that CD34$^-$KSL cells will divide in an asymmetric rather than a symmetric manner, with one daughter cell committed to lineage-specific differentiation.

A preferred model of lineage restriction proposes that nm and EM progenitor cells separately split from a common myeloid progenitor (CMP; reference 24). A multipotent CD34$^-$KSL cell never gave rise to an EM–nm colony pair throughout these studies; in effect, events predicted by the CMP model were not observed. We propose an alternative model for nm and EM lineage restrictions in the HSC compartment.

Materials and Methods

Purification of CD34$^-$KSL Cells. Bone marrow cells were obtained from 8 to 10-wk-old male C57BL/6 mice congenic for the Ly5 locus (B6-Ly5.1 mice). CD34$^-$KSL cells were purified from bone marrow cells as described previously (25). Bone marrow cells were stained with a lineage marker cocktail consisting of biotinylated anti-Gr-1, -Mac-1, -B220, -CD4, -CD8, and -Ter119 monoclonal antibodies. Lineage marker$^+$ cells were depleted using streptavidin (SA)-coupled magnetic beads (M-280; Dynal). The remaining cells were stained with FITC-conjugated anti-CD34, PE-conjugated anti-Sca-1, and allophycocyanin-conjugated anti-c-Kit antibodies, followed by development with SA–Texas red (Invitrogen). All antibodies were purchased from Becton Dickinson. Four-color analysis and sorting were performed on a FACSVantage™ SE System (Becton Dickinson). CD34$^-$KSL cells were directly sorted into a 96-well plate at 1 cell/well using a FACSVantage™ SE System. To confirm the presence of 1 cell/well, the plate was centrifuged at 1,800 revolutions/min for 5 min, placed in a 37°C incubator for at least 2 h, and observed under inverted microscopy.

Single-cell Reconstitution. A single CD34$^-$KSL cell isolated from a B6-Ly5.1 mouse was mixed with 2×10^5 bone marrow cells from a B6-Ly5.1/Ly5.2 F1 mouse. The cell mixture was injected into a B6-Ly5.2 mouse irradiated at a dose of 950 cGy. Peripheral blood cells of the recipient mice were stained with biotinylated anti-Ly5.1, FITC-conjugated anti-Ly5.2, allophycocyanin-conjugated anti-B220 antibodies, and a mixture of PE-conjugated anti–Mac-1 and anti–Gr-1 antibodies or a mixture of PE-conjugated anti-CD4 and anti-CD8 antibodies. After biotinylated antibody was developed with SA–Texas red, cells were analyzed by FACS® as described previously (25). The extent of single-cell reconstitution was expressed as (% Ly5.1 cells × 100)/(% Ly5.1 cells + % F1 cells), or percent chimerism. When percent chimerism was >1.0 for all myeloid, B-lymphoid, and T-lymphoid lineages, a test donor cell was judged to have been a long-term multilineage repopulating cell.

Single-cell Culture. Single-cell cultures of CD34$^-$KSL cells were performed as described previously (22). For induction of early cell divisions, single cells were incubated in serum-free medium (Stempro-34; Invitrogen) with 2 mM L-glutamine, 5×10^{-5} M 2-β-mercaptoethanol, and the following cytokines: 100 ng/ml of mouse SCF, 10 ng/ml of mouse IL-3, and 100 ng/ml of human TPO. For in vitro colony formation, CD34$^-$KSL cells or their progeny were individually cultured for 14 d in the same serum-free medium with SCF, IL-3, and TPO in the same concentrations as aforementioned, additionally with 10% FCS and 2 U/ml human erythropoietin (EPO). Based on colony size, the number of cells per colony was estimated to be 50–100, >100, $>10^3$, $>10^4$, or $>10^5$, followed by cell counts for representative colonies. Single-cell culture has been shown to have an advantage over conventional semisolid culture when frequencies of a variety of CFCs are to be determined. This is because the number of plated cells can be known exactly, and cells composing a colony can be efficiently collected for morphological examina-

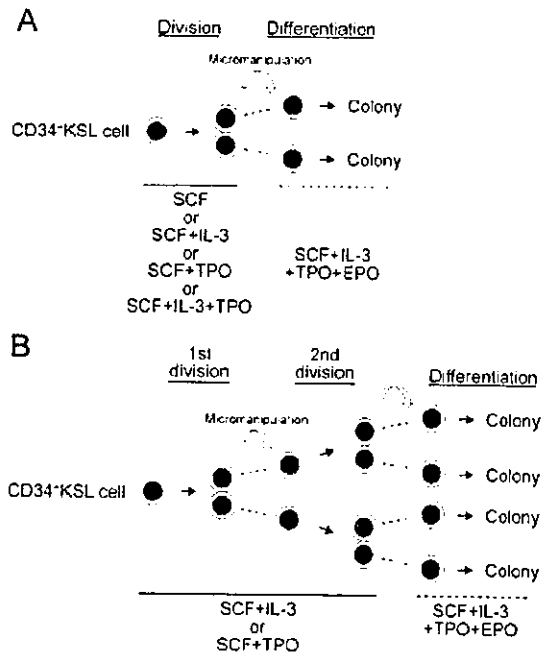

Figure 1. Micromanipulation of daughter cell pairs and granddaughter cell pairs derived from single CD34$^-$KSL cells in vitro. (A) After single CD34$^-$KSL cells underwent first divisions in the presence of SCF, SCF + IL-3, SCF + TPO, or SCF + IL-3 + TPO, members of daughter cell pairs were separated by micromanipulation and further cultured in the presence of SCF + IL-3 + TPO + EPO to permit full differentiation along myeloid lineage. (B) After single CD34$^-$KSL cells underwent first divisions in the presence of SCF + IL-3 or SCF + TPO, members of daughter cell pairs were separated into wells containing SCF + IL-3 or SCF + TPO. After each daughter cell underwent second division, granddaughter cells were separated and individually cultured in the presence of SCF + IL-3 + TPO + EPO.

tion using Cytospin (Shandon) without cross-contamination among colonies.

Micromanipulation of Daughter Cells. After single cells underwent cell division in the presence of SCF, SCF + IL-3, SCF + TPO, or SCF + IL-3 + TPO by day 5 of culture, one member of the pair of daughter cells was transferred into another well using a micromanipulator (Fig. 1 A). Individual members of daughter cell pairs, in different wells, were cultured in parallel in the presence of SCF + IL-3 + TPO + EPO for 10–14 d. For serial micromanipulation, after single cells gave rise to daughter cells in the presence of either SCF + IL-3 or SCF + TPO, one of the two daughter cells remained in the same well where culture had been initiated, and the other was transferred into a new well containing the same combination of cytokines. After daughter cells underwent cell division, the two cells derived from each daughter cell (granddaughter cells) were separated and continuously cultured in the presence of SCF + IL-3 + TPO + EPO for 10–14 d (Fig. 1 B).

Determination of Differentiation Potential. Cytospin preparations were made for all colonies consisting of ≥50 cells. Cells were stained with May-Gruenwald-Giemsa solution and morphologically identified as n, m, E, M, or blastlike (bl) cells. Two independent persons examined a total of 1,000 cells/colony in most cases; M colonies were an exception, identified in situ when 8–50 typical Ms were detected. The differentiation potential of parent cells was extrapolated backward from the differentiation potentials of daughter cells. For example, when one or two daughter cells gave rise to nmEM colonies, their parent cell was judged to have had the potential to differentiate along nmEM lineages. When one daughter cell gave rise to an nmE colony, and the other gave rise to an nmM colony, the differentiation potential of their parent cell was also considered to have been nmEM. We defined cells with nmEM differentiation potential as uncommitted cells. By contrast, commitment was defined as the event causing cells to lose the potential to differentiate along one or more lineages from among the set of n, m, E, and M. Asymmetric division was defined as cell division, resulting in production of two daughter cells with different differentiation potentials (26). To compare probabilities that asymmetric division would occur under different conditions, Fisher's exact test was used.

Table I. *Long-Term Repopulation with Single CD34⁻KSL Cells*

Repopulated lineage	No. of mice	Chimerism in Myeloid lineage	B-lymphoid lineage	T-lymphoid lineage
	(%)	%	%	%
My/B/T	8/20 (40)	53.3 ± 32.8 (n = 8)	28.4 ± 21.8	32.1 ± 23.3
My	3/20 (15)	4.1 ± 2.7 (n = 3)	–	–
B	1/20 (5)	–	1.5	–
T	1/20 (5)	–	–	8.6

A single CD34⁻KSL cell was transplanted into a lethally irradiated mouse together with 2×10^5 competitor cells. Lineage contribution was evaluated 4 mo after transplantation. All myeloid, B-lymphoid, and T-lymphoid lineages (My/B/T) were repopulated with a single cell in 8 out of 20 recipient mice. Repopulation only in myeloid (My), B-lymphoid (B), or T-lymphoid (T) lineage was also observed. Percent chimerism in each lineage is expressed as mean ± SD.

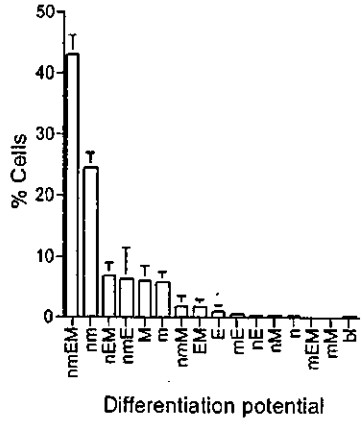

Figure 2. Colony-forming ability of single CD34⁻KSL cells. CD34⁻KSL cells were individually cultured in the presence of SCF, IL-3, TPO, and EPO for 2 wk. Percentages of CFCs with different differentiation potentials are shown based on three independent experiments. Colony cells were morphologically identified as neutrophils (n), macrophages (m), erythroblasts (E), or megakaryocytes (M). Otherwise, unidentified immature cells were designated as blastlike cells (bl). The nmEM cells constituted 43.2 ± 3.2% (mean ± SD; n = 3) of the colony-forming CD34⁻KSL cells.

Results

Long-Term Multilineage Repopulating Activity in Single CD34⁻KSL Cells. Consistent with our previous observations (22), single-cell transplantation assays identified 40% of CD34⁻KSL cells as long-term multilineage repopulating cells (Table I). In addition, 25% of the cells appeared to be myeloid, B-lymphoid, or T-lymphoid lineage-restricted repopulating cells. When CD34⁺KSL cells were used as rescue cells, 20% of the CD34⁻KSL cells contributed to long-term repopulation (21). A certain number of recipient mice died before analysis in such a rescue experiment, perhaps resulting in this lower effective reconstitution rate.

CD34⁻KSL Cells with nmEM Differentiation Potential. Colony formation by single CD34⁻KSL cells was examined in the presence of a combination of SCF + IL-3 + TPO + EPO. On average, cells were not found in 2% of the wells due to sorting failure, immediate apoptosis, or adhesion of sorted cells to the wall of the plate. The differentiation potential could not be determined in 2–3% of the cells because they gave rise either to <50 cells or to as many as 1,000 cells with bl cell morphology. The remaining cells formed a variety of colonies as shown in Fig. 2. Approximately 40% of the colonies were classified as nmEM colonies; uni-, bi-, and tripotent progenitor cells were detected less frequently. On average, 98% of the nmEM colonies consisted of $>10^4$ cells (unpublished data), suggesting that these CFCs constitute a highly proliferative subset among CD34⁻KSL cells.

Table II. *Differentiation Potentials of Paired Daughter Cells*

Cytokine	Differentiation potential: One	Differentiation potential: The other	No. of pairs
SCF	nmEM	nmEM	11
	nmEM	**nm**	4
	nmEM	**nmM**	3
	nmEM	**nEM**	2
	nmEM	**M**	2
	nmE	**EM**	1
SCF + IL-3	nmEM	nmEM	8
	nmEM	**nEM**	4
	nmEM	**nmE**	2
	nmEM	**EM**	2
	nmEM	**M**	2
	nmEM	**nmM**	1
	nmEM	**nm**	1
	nEM	**nm**	1
SCF + TPO	nmEM	nmEM	19
	nmEM	**nmE**	2
	nmEM	**nEM**	1
	nmEM	**m**	1
SCF + IL-3 + TPO	nmEM	nmEM	10
	nmEM	**nmM**	2
	nmEM	**nmE**	1
	nmEM	**nm**	1
	nmEM	**mE**	1
	nmEM	**EM**	1
	nmEM	**nE**	1
	nmEM	**M**	1
	nmE	**nmM**	1
	nEM	**mM**	1

Differentiation potential along myeloid lineage was determined for each of the members of paired daughter cells. Data on three independent experiments for each culture condition are summarized. In total, 40, 37, 52, and 41 pairs were examined after the treatment with SCF, SCF + IL-3, SCF + TPO, and SCF + IL-3 + TPO, respectively. Only the pairs whose parental cells should have had neutrophil (n), macrophage (m), erythroblast (E), and megakaryocyte (M) differentiation potential are presented. The probability of asymmetric division was 0.52 (12/23), 0.62 (13/21), 0.17 (4/23), or 0.50 (10/20) in the case of SCF, SCF + IL-3, SCF + TPO, or SCF + IL-3 + TPO, respectively. The probability of asymmetric division in the presence of SCF + IL-3 was significantly greater than that in the presence of SCF + TPO ($P = 0.0047$).

Asymmetric Division of nmEM Cells. Single $CD34^-KSL$ cells were incubated in the presence of different cytokines: SCF alone, SCF + IL-3, SCF + TPO, or SCF + IL-3 + TPO. After they divided once, the two resultant daughter cells were separated by micromanipulation (Fig. 1 A). Individual daughter cells were subsequently allowed to form colonies in the presence of SCF + IL-3 + TPO + EPO. A total of 340 daughter cells (170 pairs) were successfully micromanipulated; their differentiation potentials were then examined. Daughter cells showed a variety of differentiation potentials. The most frequently observed differentiation potential of daughter cells was nmEM, regardless of the cytokines used for induction of parent-cell division. In this work, we operationally defined retrospectively identifiable nmEM cells as HSCs and examined the differentiation potential of their immediate progeny.

Table II lists all the pairs whose parent cells were inferred to have had nmEM differentiation potential. In these cases, daughter cells (other than M-unipotent daughter cells) gave rise to colonies large enough for cytospin preparation. Two cases in which a nmEM daughter cell had no identifiable pair were excluded from analysis because a technical error in micromanipulation might have been responsible.

Regardless of what kind of cytokine mix was used, one of the two daughter cells showed differentiation potential, in most cases along nmEM lineage. These nmEM cells had tri-, bi-, and unipotent daughter cells as partners. Thus, lineage commitment in nmEM cells occurred through asymmetric division. Interestingly, progenitor cells committed to M, n, EM, or nm lineages were directly derived from nmEM cells via only one division.

When only SCF was used to induce cell division, asymmetric division took place in 52% of the cases. When IL-3 was used together with SCF, the probability of asymmetric division increased only slightly ($P = 0.62$). After an nmEM cell underwent asymmetric division in the presence of SCF alone or SCF + IL-3, one of the two daughter cells showed a variety of differentiation potentials. In contrast, when TPO was used with SCF, the number of different combinations of differentiation potential exhibited by individual pairs of daughter cells was limited, and the probability of asymmetric division dropped to 0.17. This represented a significant difference in the probability of asymmetric division between cells treated with SCF + IL-3 and cells treated with SCF + TPO ($P < 0.005$). This result is consistent with our previous observation that SCF + TPO maintained repopulating activity in pairs of daughter cells derived from single $CD34^-KSL$ cells more efficiently than did SCF + IL-3 (22). In the case of SCF + IL-3 + TPO, the probability of asymmetric division was 0.5, similar to that of SCF alone. Together, these data show that one asymmetric division of multilineage $CD34^-KSL$ cells leads to lineage commitment in their progeny and that the likelihood of asymmetric division is strongly biased by cytokine administration.

Lineage Commitment of nmEM Cells through Serial Division. To discover whether lineage commitment of nmEM cells occurs in the same manner through serial division, we examined the differentiation potential of individual granddaughter cells generated from single $CD34^-KSL$ cells in the presence of SCF + IL-3 or SCF + TPO (Fig. 1 B).

Table III. *Differentiation Potential of Paired Granddaughter Cells*

Cytokine	Differentiation potential: One	Differentiation potential: The other	No. of pairs
SCF + IL-3	nmEM	nmEM	15
	nmEM	**nm**	6
	nmEM	**mEM**	5
	nmEM	**nmM**	2
	nmEM	**nmE**	1
	nmEM	**mM**	1
	nmEM	**M**	1
	nmM	**nmE**	2
	nmM	**nEM**	1
	nm	**nEM**	2
SCF + TPO	nmEM	nmEM	21
	nmEM	**nm**	5
	nmEM	**nmM**	2
	nmEM	**nmE**	1
	nmEM	**M**	1
	nEM	**m**	1

After single CD34⁻KSL cells divided in the presence of the cytokines shown, the two daughter cells were separated. After individual daughter cells underwent division under the same condition, the granddaughter cells were again separated and were allowed to form colonies in the presence of SCF + IL-3 + TPO + EPO (Fig. 1 B). In total, 59 and 47 cell pairs generated in the presence of SCF + IL-3 and SCF + TPO were serially manipulated. Only the pairs derived from nmEM cells are presented. The probability of asymmetric division induced by SCF + IL-3 (0.58, 21/36) was significantly greater than that induced by SCF + TPO (0.32, 10/31; $P = 0.0492$).

118 and 94 paired granddaughter cells in SCF + IL-3 and SCF + TPO regimens, respectively, were successfully micromanipulated. Like daughter cells, granddaughter cells showed wide varieties of differentiation potential, but the capacity for nmEM differentiation remained most frequent. Table III shows the differentiation potentials of granddaughter cells that were considered to be derived from nmEM cells. Lineage commitment of nmEM cells also took place via asymmetric division at their second division, independent of whether IL-3 or TPO was the cytokine administered. When SCF + IL-3 were used, the second division of nmEM cells had a probability of 0.58 of generating cells asymmetric for differentiation potential. This probability was similar to that on the first division in the presence of SCF + IL-3 (Tables II and III). When SCF + TPO were used, the probability that a second division would generate cells asymmetric for differentiation potential was 0.32, higher than that on first division. Despite this increase, the difference in probability of asymmetric division between cells treated with SCF + IL-3 and cells treated with SCF + TPO remained significant. Once nmEM cells are regenerated on first division, these daughter cells behave like their parent nmEM cells.

Discussion

Precise analysis of the mode of lineage commitment in HSCs has been hampered because HSCs are very rare in the bone marrow and probably are functionally heterogeneous. Moreover, their differentiation process is mostly associated with cell division. We addressed this issue by analyzing daughter cells derived from single nmEM cells among highly purified HSCs.

The success rate of long-term reconstitution with single CD34⁻KSL cells ranged from 20 to 50% in our series of studies, presumably depending on the degree of purification in each experiment (unpublished data). As shown in Table I, 40 and 25% of the CD34⁻KSL cells were detected as multilineage and unilineage repopulating cells in this work. The seeding efficiency of repopulating cells in total appeared to be from 65 to 100%, supporting the proposition that HSCs can engraft much more efficiently than previously thought (27). By calculation, the frequency of long-term multilineage repopulating cells in this population can be corrected as 40–60%. Because >90% of the cells showed colony-forming activity (Fig. 2), most HSCs, if not all, should be able to form colonies in vitro.

To study the commitment process of HSCs while excluding from our analyses HSCs' committed progeny, we further selected for study, by retrospective inference, cells retaining the full range of capacities for differentiation (nmEM differentiation potential). The proportion of long-term repopulating cells that can be identified as nmEM progenitor cells remains uncertain. However, nmEM cells appeared to be a major subpopulation, consisting of highly proliferative cells, among CD34⁻KSL cells. Retrospectively identified nmEM cells indeed constituted a major subpopulation among CD34⁻KSL cells, but not among CD34⁺KSL cells (unpublished data).

In most daughter cell and granddaughter cell pairs, one of the two cells inherited nmEM differentiation potential from its parent cell. The other daughter or granddaughter cell either also remained capable of giving rise to an nmEM colony or became committed to some lineage (Tables II and III). These analyses relied on identification of lineage components in well-formed colonies. One of the components originally present could have been lost during the numerous cell divisions required for colony formation. In such a case, the differentiation potential of daughter cells (as assessed by identification of their descendants' phenotypes) would be underestimated. However, daughter cell pairs and granddaughter cell pairs were always assayed in parallel under exactly the same conditions. Bias owing to underestimation of differentiation potential should be equal for each of the two cells. Perhaps variation in differentiation potential between the two cells in each pair was inherent from the first division onward.

The terms "symmetric" and "asymmetric" were also defined based on components of well-formed colonies. Cell numbers and differential counts within colonies were not taken into account when evaluating lineage commitment. The pioneer work on paired daughter cells done by Suda et al. has suggested the progressive and stochastic lineage restriction of HSCs (8, 9). Suda et al. also have observed that multipotent cells asymmetrically give rise to unipotent cells. It has been shown that these blast colonies contain very few long-term repopulating cells (28). Their observations likely reflect the behavior of progenitor cells at an early stage of differentiation. Together, our data suggest that HSCs and their early progeny similarly undergo lineage commitment in an asymmetric manner.

The *Drosophila melanogaster* neuroblast asymmetrically divides to produce both neuroblast and ganglion mother cell (26). This similarity to mouse HSC behavior suggests that asymmetric division is a mechanism for generating cellular diversity common to stem and progenitor cells in the nervous and hematopoietic systems. Asymmetric division is considered to involve both unequal segregation of determinants and cell–cell interaction (26). Numb protein has been implicated as one such determinant in neural development. The primary function of Numb seems not the direct specification of fate, but rather modulation of environmental cues like Notch signaling (29). Although such a determinant has not been recognized in hematopoietic systems, a distinct expression pattern of particular genes in one of the two daughter cells may lead to lineage commitment as proposed by Cross et al. (30): different regions of the cell sap at the moment of division may contain unequally distributed gene products, and this inequality in distribution may tip the balance from one commitment pattern to another.

Expression of transcriptional factors such as SCL, GATA-2, Gfi-1B, and PU.1 has been detected in $CD34^-KSL$ cells (31, 32). If all these genes are expressed in a daughter cell, that cell may retain nmEM differentiation potential. If PU.1 is predominantly expressed, a daughter cell may commit to nm lineage. In contrast, a daughter cell may commit to EM lineage if expression levels of SCL, GATA-2, and Gfi-1B in concert dominate PU.1. Cross-antagonism can be an alternative mechanism for dominant action of a certain transcriptional factor over an opposing one (33).

This work clearly demonstrates an instructive role of cytokines in lineage commitment at the level of HSCs (Tables II and III). The probability of lineage commitment by nmEM cells in the presence of SCF + TPO was significantly lower than that in the presence of SCF + IL-3. The probability remained similar through the initial two divisions with SCF + IL-3 (0.62 and 0.58), but not with SCF + TPO (0.17 and 0.32). Lineage commitment by HSCs can be controlled to some extent by external factors. Whether cytokines also influence which lineage potential is chosen by HSCs upon their lineage commitment remains unclear. Fig. 3 presents the numbers of committed progenitor cells that appeared after the first and second divisions of nmEM cells. In the presence of either IL-3 or TPO,

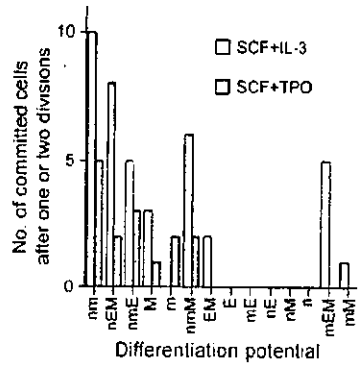

Figure 3. Distribution of lineage-committed daughter and granddaughter cells. The numbers of daughter and granddaughter cells that lost the capacity to differentiate along one or more lineages are graphed, using data in Tables II and III. All possible combinations of differentiation potential are shown in the same order as that presented in Fig. 2.

nmEM cells seemed to have a preference in lineage choice, suggesting that the fate decision of HSCs is not a random event. Alternatively, this may simply indicate postcommitment selection in given culture conditions.

Interestingly, we did not observe the combination of nm lineage and EM lineage in a total of 154 pairs of daughter and granddaughter cells (Tables II and III). A CMP has been described as giving rise to separate colonies of nm lineage and EM lineage in culture, with EM lineage–committed progenitors, in turn, giving rise to E lineage–committed progenitors and M lineage–committed progenitors, supporting a progressive loss of differentiation potential (34). Our data suggest an alternative pathway of myeloerythroid differentiation in which nm or EM progenitor cells can asymmetrically develop from an HSC population

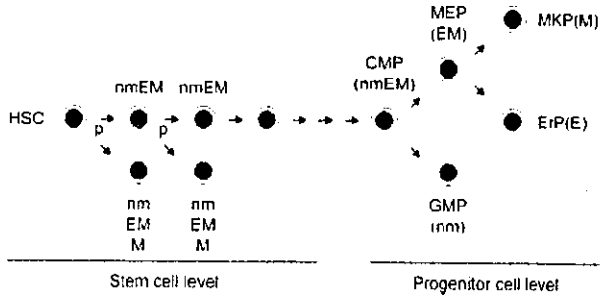

Figure 4. Myeloid lineage restriction model. The mode of lineage commitment at the level of HSCs may differ from that at the level of progenitor cells. Our model for HSCs is presented in combination with the model proposed by Weissman's group (34). An HSC can directly give rise to lineage-committed progenitor cells such as nm, EM, or M progenitor cells through initial HSC division in asymmetric manner. It may give rise to a common myeloid progenitor (CMP) after a certain number of divisions. The CMP gives rise to a megakaryocyte/erythrocyte lineage–restricted progenitor (MEP) and to a granulocyte/macrophage lineage-restricted progenitor (GMP). The MEP progressively gives rise to a megakaryocyte-committed progenitor (MKP) and to an erythrocyte lineage-committed progenitor (ErP). P, probability of asymmetric division.

with no need for a CMP intermediate (Fig. 4). The modes of lineage commitment possibly differ between stem and progenitor cell compartments.

HSCs, progenitor cells of CMPs and common lymphoid progenitors, and CMPs could have all been detected as nmEM cells in this work because self-renewal activity and B- and T-lymphoid differentiation potentials were not examined. In the presence of SCF + TPO, 42 out of 46 daughter cells (91%) and 51 out of 62 granddaughter cells (82%) retained the capacity to differentiate along nmEM lineage after, respectively, their first and second divisions (Tables II and III). The nmEM cells apparently regenerated themselves in their early divisions. On the other hand, a substantial loss in the number of long-term repopulating cells under the same conditions has been observed (22). It is assumed that a majority of nmEM cells generated in culture in this work might have lost self-renewal activity, but still maintained the capacity to differentiate along multiple lineages. Common progenitor cells giving rise to both CMPs and common lymphoid progenitors have not been identified. After a certain number of divisions, HSCs should give rise to such progenitor cells at a certain stage of differentiation. To verify our model of lineage commitment, both myeloid and lymphoid differentiation potentials should be examined for intermediate cells between HSCs and CMPs at the clonal level. To do this, an assay sensitive and efficient enough for detection of all potentials in individual cells needs to be developed. Our working model, nonetheless, may help in studying the molecular mechanism of lineage commitment in HSCs.

The authors thank K. Fujii and T. Suda for helpful discussion and A.S. Knisely for critical reading of the manuscript.

This work was supported by grants from the Ministry of Education, Culture, Sports, Science and Technology.

Submitted: 6 June 2003
Accepted: 20 November 2003

References

1. Lansdorp, P.M. 1997. Self-renewal of stem cells. *Biol. Blood Marrow Transplant.* 3:171–178.
2. Metcalf, D. 1998. Lineage commitment and maturation in hematopoietic cells: The case for extrinsic regulation. *Blood.* 92:354–352.
3. Ogawa, M. 1999. Stochastic model revisited. *Int. J. Hematol.* 69:2–5.
4. Weissman, I.L. 2000. Stem cells: Units of development, units of regeneration, and units in evolution. *Cell.* 100:157–168.
5. Till, J.E., E.A. McCulloch, and L. Siminovitch. 1964. A stochastic model of stem cell proliferation, based on the growth of spleen colony-forming cells. *Proc. Natl. Acad. Sci. USA.* 51:29–36.
6. Humphries, R.K., A.C. Eaves, and C.J. Eaves. 1981. Self-renewal of hemopoietic stem cells during mixed colony formation in vitro. *Proc. Natl. Acad. Sci. USA.* 78:3629–3633.
7. Nakahata, T., A.J. Gross, and M. Ogawa. 1982. A stochastic model of self-renewal and commitment to differentiation of the primitive hemopoietic stem cells in culture. *J. Cell. Physiol.* 113:455–458.
8. Suda, T., J. Suda, and M. Ogawa. 1984. Disparate differentiation in mouse hemopoietic colonies derived from paired progenitors. *Proc. Natl. Acad. Sci. USA.* 81:2520–2524.
9. Suda, J., T. Suda, and M. Ogawa. 1984. Analysis of differentiation of mouse hemopoietic stem cells in culture by sequential replating of paired progenitors. *Blood.* 64:393–399.
10. Leary, A.G., L.C. Strauss, C.I. Civin, and M. Ogawa. 1985. Disparate differentiation in hemopoietic colonies derived from human paired progenitors. *Blood.* 66:327–332.
11. Tsuji, K., and T. Nakahata. 1989. Stochastic model for multipotent hemopoietic progenitor differentiation. *J. Cell. Physiol.* 139:647–653.
12. Mayani, H., W. Dragowska, and P.M. Landsdorp. 1993. Lineage commitment in human hemopoiesis involves asymmetric cell division of multipotent progenitors and does not appear to be influenced by cytokines. *J. Cell. Physiol.* 157: 576–586.
13. Brummendorf, T.H., W. Dragowska, J.M.J.M. Zijlmans, G. Thornbury, and P.M. Lansdorp. 1998. Asymmetric cell divisions sustain long-term hematopoiesis from single-sorted human fetal liver cells. *J. Exp. Med.* 188:1117–1124.
14. Suda, T., J. Suda, M. Ogawa, and J.N. Ihle. 1985. Permissive role of interleukin 3 (IL-3) in proliferation and differentiation of multipotential hemopoietic progenitors in culture. *J. Cell. Physiol.* 124:182–190.
15. Stoffel, R., S. Ziegler, N. Ghilardi, B. Ledermann, F.J. deSauvage, and R.C. Skoda. 1999. Permissive role of thrombopoietin and granulocyte colony-stimulating factor receptors in hematopoietic cell fate decisions in vivo. *Proc. Natl. Acad. Sci. USA.* 96:698–702.
16. Wolf, N.S., and J.J. Trentin. 1975. The restorative effect of erythropoietic stimulation upon the sublethally irradiated (SIL) hematopoietic stem and/or its progeny. *Exp. Hematol.* 3:57–64.
17. Van Zant, G., and E. Goldwasser. 1979. Competition between erythropoietin and colony-stimulating factor for target cells in mouse marrow. *Blood.* 53:946–965.
18. Metcalf, D., and A.W. Burgess. 1982. Clonal analysis of progenitor cell commitment to granulocyte or macrophage production. *J. Cell. Physiol.* 111:275–283.
19. Metcalf, D. 1991. Lineage commitment of hemopoietic progenitor cells in developing blast cell colonies: Influence of colony-stimulating factors. *Proc. Natl. Acad. Sci. USA.* 88: 11310–11314.
20. Metcalf, D. 1998. Lineage commitment in the progeny of murine hematopoietic preprogenitor cells: Influence of thrombopoietin and interleukin 5. *Proc. Natl. Acad. Sci. USA.* 95: 6408–6412.
21. Osawa, M., K.-i. Hanada, H. Hamada, and H. Nakauchi. 1996. Long-term lymphohematopoietic reconstitution by a single CD34-low/negative hematopoietic stem cell. *Science.* 273:242–245.
22. Ema, H., H. Takano, K. Sudo, and H. Nakauchi. 2000. In vitro self-renewal division of hematopoietic stem cells. *J. Exp. Med.* 192:1281–1288.
23. Nakauchi, H., K. Sudo, and H. Ema. 2000. Quantitative assessment of the stem cell self-renewal capacity. *Ann. NY Acad. Sci.* 938:18–24.
24. Akashi, K., D. Traver, T. Miyamoto, and I.L. Weissman. 2000. A clonogenic common myeloid progenitor that gives rise to all myeloid lineages. *Nature.* 404:193–197.
25. Sudo, K., H. Ema, Y. Morita, and H. Nakauchi. 2000. Age-

associated characteristics of murine hematopoietic stem cells. *J. Exp. Med.* 192:1273–1280.
26. Jan, Y.N., and L.Y. Jan. 2001. Asymmetric cell division in the *Drosophila* nervous system. *Nat. Rev. Neurosci.* 2:772–779.
27. Benveniste, P., C. Cantin, D. Hyam, and N.N. Iscove. 2003. Hematopoietic stem cells engraft in mice with absolute efficiency. *Nat. Immunol.* 4:708–713.
28. Tsunoda, J., S. Okada, J. Suda, K. Nagayoshi, H. Nakauchi, K. Hatake, Y. Miura, and T. Suda. 1991. In vivo stem cell function of interleukin-3-induced blast cells. *Blood.* 78:318–322.
29. Cayouette, M., and M. Raff. 2002. Asymmetric segregation of Numb: a mechanism for neural specification from *Drosophila* to mammals. *Nat. Neurosci.* 5:1265–1269.
30. Cross, M.A., and T. Enver. 1997. The lineage commitment of haemopoietic progenitor cells. *Curr. Opin. Genet. Dev.* 7:609–613.
31. Nakauchi, H., H. Takano, H. Ema, and M. Osawa. 1999. Further characterization of CD34-low/negative mouse hematopoietic stem cells. *Ann. NY Acad. Sci.* 872:57–66.
32. Osawa, M., T. Yamaguchi, Y. Nakamura, S. Kaneko, M. Onodera, K. Sawada, A. Jegalian, H. Wu, H. Nakauchi, and A. Iwama. 2002. Erythroid expansion mediated by the Gfi-1B zinc finger protein: role in normal hematopoiesis. *Blood.* 100:2769–2777.
33. Cantor, A.B., and S.H. Orkin. 2001. Hematopoietic development: a balancing act. *Curr. Opin. Genet. Dev.* 11:513–519.
34. Nakorn, T.N., T. Miyamoto, and I.L. Weissman. 2003. Characterization of mouse clonogenic megakaryocyte progenitors. *Proc. Natl. Acad. Sci. USA.* 100:205–210.

MOLECULAR AND CELLULAR BIOLOGY, May 2004, p. 4207–4220 Vol. 24, No. 10
0270-7306/04/$08.00+0 DOI: 10.1128/MCB.24.10.4207–4220.2004

The *Sox-2* Regulatory Regions Display Their Activities in Two Distinct Types of Multipotent Stem Cells

Satoru Miyagi,[1,2] Tetsuichiro Saito,[3] Ken-ichi Mizutani,[3] Norihisa Masuyama,[4] Yukiko Gotoh,[4] Atsushi Iwama,[5] Hiromitsu Nakauchi,[5] Shinji Masui,[6] Hitoshi Niwa,[6] Masazumi Nishimoto,[1] Masami Muramatsu,[1] and Akihiko Okuda[1]*

Division of Developmental Biology, Research Center for Genomic Medicine, Saitama Medical School, Saitama 350-1241,[1] REDS Group, Saitama Small Enterprise Promotion Corporation, Skip City, Kawaguchi, Saitama 333-0844,[2] Department of Development and Differentiation, Institute for Frontier Medical Sciences, Kyoto University, Kyoto 606-8507,[3] Institute of Molecular and Cellular Biosciences, University of Tokyo, Tokyo 113-0032,[4] Laboratory of Stem Cell Therapy, Center for Experimental Medicine, Institute of Medical Science, University of Tokyo, Tokyo 108-8639,[5] and Laboratory for Cell Pluripotency Studies, RIKEN, Center for Developmental Biology, Chuo-ku, Kobe 650-0047,[6] Japan

Received 4 November 2003/Returned for modification 8 January 2004/Accepted 18 February 2004

The *Sox-2* gene is expressed in embryonic stem (ES) cells and neural stem cells. Two transcription enhancer regions, Sox-2 regulatory region 1 (SRR1) and SRR2, were described previously based on their activities in ES cells. Here, we demonstrate that these regulatory regions also exert their activities in neural stem cells. Moreover, our data reveal that, as in ES cells, both SRR1 and SRR2 show their activities rather specifically in multipotent neural stem or progenitor cells but cease to function in differentiated cells, such as postmitotic neurons. Systematic deletion and mutation analyses showed that the same or at least overlapping DNA elements of SRR2 are involved in its activity in both ES and neural stem or progenitor cells. Thus, SRR2 is the first example of an enhancer in which a single regulatory core sequence is involved in multipotent-state-specific expression in two different stem cells, i.e., ES and neural stem cells.

Stem cells have been identified in various organs, including hematopoietic tissue and the nervous system, and play a central role in tissue generation during development (for details, see references 22, 49, and 53). These stem cells are also present in adult animals, where they participate in tissue repair and the homeostasis of each tissue. Stem cells share the properties of self-renewal and the ability to generate at least one (but usually more) differentiated cell types, suggesting the presence of common genetic programs to maintain these unique biological properties of stem cells. To date, an increasing amount of data from global transcriptional profiling analyses have piled up (10, 15, 19, 36, 45, 50), and these analyses have led to the identification of a number of genes which are commonly expressed in more than two different types of stem cells. Indeed, some, such as the *integrin alpha 6* and *polycystic kidney disease 2* genes, have been shown to be expressed in all of the three best-characterized types of stem cells, i.e., embryonic stem (ES) cells, neural stem cells, and hematopoietic stem cells (15, 36). However, it is not known whether the expression of these genes is supported by a single regulatory enhancer which operates in different types of stem cells or whether such expression merely reflects the combined actions of multiple different regulatory regions in which individual regulatory enhancers function only in specific stem cells. Recently, Cairns et al. (7) demonstrated that a portion of the first intron of the *c-kit* gene supports its expression in both hematopoietic and germ cell lineages. However, because the enhancer region was not finely mapped, it is not known at present whether a single regulatory sequence indeed participates in gene expression in these two different cell lineages.

Sox-2, a transcriptional factor bearing a high-mobility-group box, is one of the examples expressed in more than two different types of stem cells (4, 57). In fact, zygotically transcribed Sox-2 mRNA is detected in the inner cell mass, epiblasts, and germ cells in early mouse embryos. *Sox-2* is also expressed in trophoblast stem cells, which correspond to the stem cells of extraembryonic ectodermal tissues (4). In these cell lineages, *Sox-2* expression is restricted to cells with stem cell characteristics and no longer expressed in cells with restricted developmental potential. Besides being expressed in early mouse embryos, *Sox-2* is also expressed in the developing central nervous system (6, 12, 20, 34, 51, 52, 57). *Sox-2* expression is first detected uniformly in the neural plate, in which most of the cells are multipotent. However, once the columnar epithelium of the neural plate acquires a more complex stratum structure, the expression becomes restricted to the germinal layer, where multipotent neural stem cells are enriched. Moreover, Graham et al. (11) recently demonstrated that the signaling of members of the SoxB1 transcription factor group, which includes the Sox-2 protein, is sufficient to maintain the panneural properties of neural progenitor cells.

Recent microarray analyses have pointed out significant similarities between ES cells and neural stem cells at the transcriptional level (36). Therefore, it is assumed that the ways of supporting stem cell-specific gene expression in these two dis-

* Corresponding author. Mailing address: Division of Developmental Biology, Research Center for Genomic Medicine, Saitama Medical School, 1397-1 Yamane Hidaka, Saitama 350-1241, Japan. Phone: 81-429-85-7268. Fax: 81-429-85-7264. E-mail: akiokuda@saitama-med.ac.jp.

tinct types of stem cells are intimately related and that at least some of the genes whose expressions overlap in ES and neural stem cells are regulated by common enhancers which function in these two distinct stem cells. We pursued the possibility that the *Sox-2* gene possesses such a regulatory region(s).

The two regulatory regions termed Sox-2 regulatory region 1 (SRR1) and SRR2, which were identified based on their activities in pluripotent ES cells, were reported previously (48). Moreover, it was shown that SRR2 has a regulatory core sequence comprising octamer and Sox-2 binding sequences and that SRR2 exhibits its activity by recruiting the Oct-3/4–Sox-2 or Oct-6–Sox-2 complex to it in ES cells. In this report, we demonstrate that both SRR1 and SRR2 also exert their activities in neural stem cells. We also show that SRR2 utilizes the same core sequence to support its multipotent-state-specific enhancer activity in both ES and neural stem cells.

MATERIALS AND METHODS

Plasmid constructions. For constructing β-*geo* reporter plasmids (see Fig. 2), the splice acceptor portion of the *engrailed* gene and internal ribosome entry site (IRES) region were removed from pGT1.8IresBgeo (27) and either SRR1 or SRR2 was subcloned together with a herpes simplex virus thymidine kinase (*tk*) promoter (positions −109 to +51) (21). SRR1 and SRR2 encompass the regions from positions −3937 to −3487 and +3641 to +4023 of *Sox-2* genomic DNA, respectively, in which the transcription start site is considered position +1 (see reference 54). The location of SRR1 has been narrowed down to this short region (451 bp) (S.M. and A.O., unpublished data) from previous work (48). SRR1 was recovered by PCR, while the SRR2 portion was obtained from cloned genomic DNA.

For constructing the ptk-Venus reporter plasmids shown in Fig. 3A, the second intron enhancer of the rat *nestin* gene (+1162 to +1798) (17) was amplified by PCR. As for SRR1 and SRR2, the same DNA fragments used to obtain the results shown in Fig. 2 were used. These regulatory regions were subcloned into the SalI/NcoI site of Venus/pCS2 (28), which carries the *Venus* reporter gene together with the *tk* promoter with the aid of linkers. Venus is a modified form of enhanced yellow fluorescent protein bearing a unique set of amino acid substitutions (F46L, F64L, M153T, V163A, and S175G) and exhibits enhanced fluorescence because of these mutations (28). For constructing EF1-Venus, the *EF1* promoter region was recovered from the pEF-BOS vector (26) and subcloned into the SalI/NcoI site of Venus/pCS2. The internal deletion and nucleotide substitution mutants of SRR2 shown in Fig. 7A were all obtained by PCR-based procedures in which mut*Oct* and mut*Sox* carried the same mutations of triple-point mutants 19 and 16, respectively, which were described previously (48). For constructing the 4×CORE plasmid, the SRR2 core sequence, 5′-GG CAGCCATTGTGATGCA TATGGATTA-3′, was multimerized to four copies according to the method of Nishimoto et al. (30) and subcloned into the SalI/NcoI site of the *Venus* reporter together with the *tk* promoter.

For constructing the *puro-Venus* reporter gene, coding regions of these two protein were fused with the aid of a linker and subcloned into the plasmid bearing the polyadenylation sequence from the *PGK* gene (S.M. and H.N., unpublished data). Subsequently, various regulatory regions used to obtain the results shown in Fig. 4A and B were individually subcloned into the vector.

All expression vectors of octamer factors and the Sox-2 protein were constructed by subcloning cDNAs carrying entire coding regions of these proteins into the EcoRI site of the pCAG vector (31), while construction of the SRR2/tk-luciferase reporter gene was described previously (48).

ES cell culture and transfection. E14 ES cells were cultured as described previously (29). The β-*geo* reporter plasmid bearing SRR1 or SRR2 was introduced into ES cells by electroporation according to the method of Thomas and Capecchi (46). After selection with G418, the drug-resistant clones were picked and expanded for subsequent analyses.

In vitro differentiation of ES cells. Neural differentiation of ES cells was performed essentially as described by Bain et al. (5). Briefly, E14 ES cells were cultured as usual on a feeder layer with leukemia inhibitory factor-supplemented medium. Subsequently, embryoid bodies were generated by culturing cells in bacterial-grade dishes. These embryoid bodies were maintained as a suspension culture for 8 days, and cells were exposed to all-*trans*-retinoic acids (0.5 μM) for the last 4 days. Subsequently, cell aggregates were plated onto tissue culture dishes precoated with poly-D-lysine (PDL) and laminin and cultured for another 2 days before being subjected to immunohistochemical analyses. Establishment and culture of trophoblast stem cells by cultivating ZHTc4 ES cells with FGF-4, heparin, and tetracycline were done as described by Niwa et al. (32).

Neurosphere culture. Neurospheres were generated from an embryonic day 13.5 (E13.5) or E17.5 mouse forebrain according to the method of Reynolds et al. (38), with slight modifications utilizing B-27 supplement (Invitrogen), 20 ng of epidermal growth factor (Becton Dickinson) per ml, and 20 ng of basic fibroblast growth factor (Roche) per ml in place of a defined hormone mix and salt mixture.

Generation of lentivirus vectors and infection of neurosphere and hematopoietic stem cells. For constructing self-inactivating vector plasmids used to obtain the results shown in Fig. 1 and 4C, pCS-CDF-CG-PRE, a modified form of pCS-CG-PRE (43), was used as starting material. pCS-CDF-CG-PRE carries a polypurine tract which increases the efficiency of infection (H. Miyoshi, unpublished data). First, the cytomegalovirus promoter and green fluorescent protein (GFP) cDNA portions were removed from the plasmid, and *Venus* reporter cassettes connected to one of the regulatory regions shown in Fig. 1 were then subcloned. For the *UTF1* regulatory region, the genomic DNA region from +991 to +2041 (29) was used, while for all other regulatory regions, the same portions used for constructing *Venus* reporter plasmids were used. The production of pseudotyped human immunodeficiency virus type 1-based lentivirus possessing vesicular stomatitis virus G protein (VSV-G) was carried out according to the method of Miyoshi et al. (25) in which the VSV-G protein allows the virus to infect mammalian cells in general (for details, see references 24 and 25). The vector titers were determined as described by Tahara-Hanaoka et al. (43).

For infecting lentivirus, neurospheres were dissociated and immediately infected with the virus at a multiplicity of infection of 1.0. Under this condition, about 70% of neurosphere cells were infected. These cells were cultured for another 3 days in serum-free medium containing appropriate growth factors so that the cells could maintain a multipotent state as described above or in medium containing 10% fetal bovine serum (FBS).

Murine hematopoietic stem cells with a $CD34^{-/low}$ c-Kit^+ $Sca\text{-}1^+$ Lin^- phenotype ($CD34^-$ KSL) were prepared from bone marrow cells according to the method of Osawa et al. (33). Briefly, bone marrow cells were obtained from the tibias and femurs of C57BL/6 mice. These bone marrow cells were overlaid with sodium metrizoate, and low-density cells were harvested. Lineage-positive cells were removed from these cells by utilizing biotinylated antilineage markers (Mac1, Gr-1, B220, CD4, CD8, and TER119), and $CD34^{-/low}$ c-Kit^+ $Sca\text{-}1^+$ cells were sorted by fluorescence-activated cell sorting with a Vantage SE (Becton Dickinson). These hematopoietic stem cell-enriched cells were transduced with lentivirus bearing the *Venus* reporter gene at a multiplicity of infection of 300 as described by Tahara-Hanaoka et al. (43). Under these conditions, about 50% of $CD34^-$ KSL cells were infected.

In utero electroporation. Gene transfer into the developing mouse brains and subsequent analyses were done as described by Saito and Nakatsuji (40). ICR strain mice were used for the analyses. Data shown in Fig. 7B were obtained with coinjection of one of the Venus reporter plasmids shown in Fig. 7A with an internal control DsRed reporter plasmid in which DsRed expression is supported by the chicken β-actin promoter (31). In all cases, 3 μl of solution containing 0.1 pmol of DNA was injected.

Immunostaining. Indirect immunocytochemistry was carried out with cells that had been cultured on coverslips (for in vitro-differentiated ES cells) or in slide chambers (for clonally grown neurospheres) coated with PDL and laminin. Cells were fixed with 4% paraformaldehyde for 20 min at room temperature. For immunohistochemical analyses, brains were recovered from 17.5-day-postcoitum (d.p.c.) embryos in which the SRR2/tk-Venus reporter had been introduced at 13.5 d.p.c. by in utero electroporation and embedded in OCT materials after fixation with 4% paraformaldehyde. The frozen sections (thickness, 20 μm) of fetal brains were incubated with anti-nestin, MAP2, or phosphohistone H3 antibody together with anti-GFP antibody. Immunostaining was performed as described by Saba et al. (39) with appropriate Alexa Fluor dye-conjugated secondary antibodies from Molecular Probes.

Antibodies. The following antibodies were used for immunostaining analyses: anti-Sox-2 (rabbit immunoglobulin G [IgG]; CHEMICON), anti-phosphohistone H3 (clone 6G3; Cell Signaling Technology), anti-MAP2 (clone HM-2; Sigma), anti-glial fibrillary acidic protein (anti-GFAP) (rabbit IgG; Sigma), O4 (clone 81; CHEMICON), antinestin (clone Rat401; BD PharMingen), anti-GFP (rabbit antiserum; MBL), and anti-β-galactosidase (anti-β-Gal) (rabbit IgG; Cappel). These antibodies were diluted appropriately according to the suppliers' recommendations.

Luciferase assay. COS cells in 60-mm-diameter dishes were transfected by lipofection using lipofectamine 2000 (Invitrogen) with the amounts of reporter and expression vectors indicated in the legend to Fig. 7. The total amount of

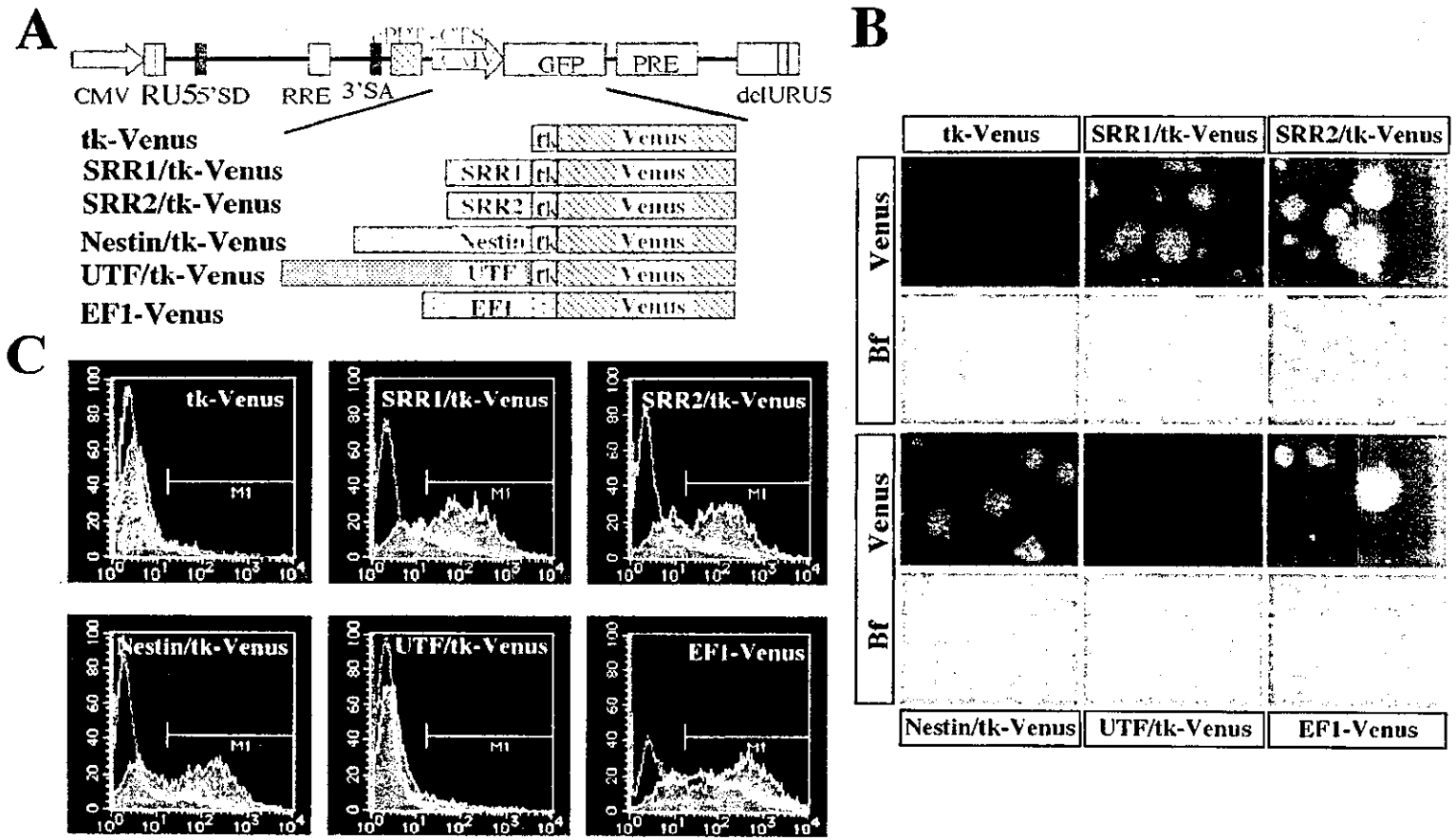

FIG. 1. SRR1 and SRR2 show enhancer activities equivalent to that of the *nestin* regulatory region in neurospheres. (A) Schematic representation of the self-inactivating vector (pCS-CDF-CG-PRE) and *Venus* reporter genes bearing distinct regulatory regions. The exact coordinate of each regulatory enhancer in the original gene locus is described in Materials and Methods. Abbreviations used are as follows: CMV RU5, the 5′ long terminal repeat of the human immunodeficiency virus in which the U3 enhancer-promoter region is replaced by the cytomegalovirus promoter; 5′SD, splice donor site; RRE, *rev* responsive element; 3′SA, splice acceptor site; cPPT, central polypurine tract; CTS, central termination sequence; PRE, woodchuck hepatitis virus posttranscriptional regulatory element; and delURU5, 3′ long terminal repeat lacking the enhancer-promoter portion of U3. (B) Functional analyses of SRR1 and SRR2 in forebrain-derived neurospheres. At 72 h postinfection with lentiviruses, reporter gene expression in neurosphere cells was examined under a fluorescence microscope as well as in bright fields (Bf). (C) Both SRR1 and SRR2 show the enhancer activities rather specifically in neural stem or progenitor cell populations. Neurosphere cells were infected with lentiviruses as described for panel B and maintained in the multipotent state or induced to differentiate with FBS. These cells were then dissociated to the single-cell level, and Venus expression was quantitated on a FACSCalibur device. The green portion and the orange line correspond to data obtained from a neural stem or progenitor cell population and differentiation-induced cells, respectively. The numbers in vertical and horizontal axes represent cell counts and Venus fluorescence intensity, respectively.

DNA was adjusted to 8 μg with pUC18. After 48 h of transfection, transcription levels were determined by the dual-luciferase system according to the instructions of the manufacturer (Promega).

RESULTS

SRR1 and SRR2 exert their activities in forebrain-derived neurosphere cells. The *Sox-2* gene is expressed in various types of stem cells, including ES cells and neural stem cells (4, 35, 56, 57). Since two regulatory regions, SRR1 and SRR2, which are involved in the expression of the *Sox-2* gene in pluripotent ES cells, have already been identified (48), we examined whether these regulatory regions also work in multipotent neural stem cells. We first produced lentiviruses carrying the *Venus* reporter gene, which encodes a fluorescent protein that exhibits enhanced fluorescence (28), and one of the various regulatory regions shown in Fig. 1A. We then used these viruses to infect cells from neurosphere colonies which had been generated from the forebrains of 13.5-d.p.c. mouse embryos. Culture continued for another 72 h. As expected, the *EF1* promoter and *nestin* enhancer, the best-characterized neural stem cell- or progenitor cell-specific enhancer (17), were active and drove the transcription of the *Venus* reporter gene in the majority of neurosphere cells (Fig. 1B). More importantly, a substantial number of cells also became Venus positive when these cells were infected with viruses bearing SRR1 or SRR2, whereas the *tk* promoter alone or the ES cell-specific regulatory element of the *UTF1* gene (29) did not show any obvious effect. To evaluate the strength of these regulatory regions on reporter gene expression, these neurosphere cells were dissociated and their fluorescent intensity was quantitated by fluorescence-activated cell sorting analysis. These analyses revealed that SRR1 and SRR2 display activities equivalent to that of the *nestin* enhancer (Fig. 1C). From these results, we concluded that both SRR1 and SRR2 are able to function in neural stem cell-enriched neural cells. We also confirmed that these regulatory regions, like the *nestin* enhancer, do not have a prominent effect on reporter gene expression when cells were cultured under differentiation-inducing conditions (Fig. 1C), indicating that both SRR1 and SRR2 display their activities rather specifically in multipotent neural stem and progenitor cell populations.

SRR1 and SRR2 direct β-*geo* reporter gene expression in *nestin*-positive cells derived from ES cells. To further characterize the specificities of SRR1 and SRR2 activities in neural cells, we took advantage of their activities in pluripotent ES cells. That is, we made two *tk* promoter/β-*geo* reporter constructs in which either SRR1 or SRR2 is connected to the promoter. These plasmids were introduced into ES cells by electroporation, and stable transformants were obtained. These cells were subjected to neural differentiation in which cells are cultured as embryoid bodies for 4 days in the absence of retinoic acids and then cultured for another 4 days in the presence of retinoic acids (see Materials and Methods). It should be noted that ES cell-specific enhancers, such as that of the *UTF1* gene, lost their entire activity during this procedure and that the activities of both SRR1 and SRR2 also profoundly diminished within the first 4 days of this procedure (data not shown). We then examined whether SRR1 and SRR2, whose activities decreased in the beginning of the process, were reactivated when complete neural differentiation procedures were applied to the cells. We performed immunological staining procedures with these differentiation-induced cells to compare the expression profiles of β-Gal directed by SRR1 or SRR2 and endogenous neural-lineage cell markers. As shown in Fig. 2A, we found that the expression of β-Gal in cells in which SRR1 directed β-Gal protein production significantly overlapped that in cells possessing nestin, but the protein was not detected in cells with MAP2, one of the markers for postmitotic neurons. We obtained essentially the same results with SRR2 (Fig. 2B). Moreover, as shown in Fig. 2C, we confirmed the completely mutually exclusive patterns of expression of β-Gal directed by SRR2 and MAP2 with the aid of confocal microscopy. To determine the extent of coexpression of the β-Gal and nestin proteins more precisely, cells bearing the SRR2/β-Gal transgene were disaggregated after induction of neural differentiation and then immunostained. A representative example is shown in Fig. 2D. We found that about 96% of β-Gal-positive cells were also positive for nestin. Likewise, 94% of β-Gal-positive cells were positive for nestin when cells bearing the SRR1/β-Gal transgene were used (data not shown). Thus, these results also indicate that both SRR1 and SRR2 exert their functions rather specifically in neural stem and progenitor cells but not in postmitotic neurons.

SRR1 and SRR2 display their enhancer activities rather specifically in cells located in the ventricular zone of the developing brain. Next, we examined whether SRR1 and SRR2 are able to function in developing brains of mouse embryos. We employed in utero electroporation, by which DNAs injected into the lateral or third ventricle of the mouse embryo brain are efficiently delivered into brain cells (40). We introduced the *Venus* reporter plasmids shown in Fig. 3A into the brains of 13.5-d.p.c. mice and maintained them in the uterus. Four days after electroporation, the brains were recovered, sliced with a vibratome, and viewed under a fluorescence microscope. By this method, DNA is delivered exclusively into cells facing the ventricle, which are mainly neural stem or progenitor cells. While neural stem cells make cell division in the ventricular zone, some of their descendants, postmitotic neurons, migrate into the cortical plate. As expected, many cells in both the cortical plate and the ventricular zone were labeled by the transfection of EF1-Venus, in which process *Venus* expression is driven by the generally active *EF1* promoter. In contrast, the transfection of SRR2/tk-Venus labeled mainly the ventricular zone and only a limited number of cells in the cortical plate, indicating that the transcriptional stimulating activity of SRR2 in neural stem or progenitor cells declined abruptly when cells differentiated and migrated to the cortical plate portion. This assumption was supported by the fact that Nestin/tk-Venus also gave essentially the same *Venus* expression pattern. SRR1 also supported ventricular-zone-specific *Venus* expression, albeit rather weakly compared with what occurred with SRR2 and the *nestin* enhancer. As expected, cells with the *tk* promoter alone and those with the *UTF1* enhancer could not produce appreciable amounts of Venus-positive cells in these assays (data not shown).

SRR1 and SRR2 do not exert their enhancer activities in trophoblast and hematopoietic stem cells. *Sox-2* expression is not restricted to ES cells and neural stem cells; it is also expressed in trophoblast stem cells (4, 55). Moreover, it has

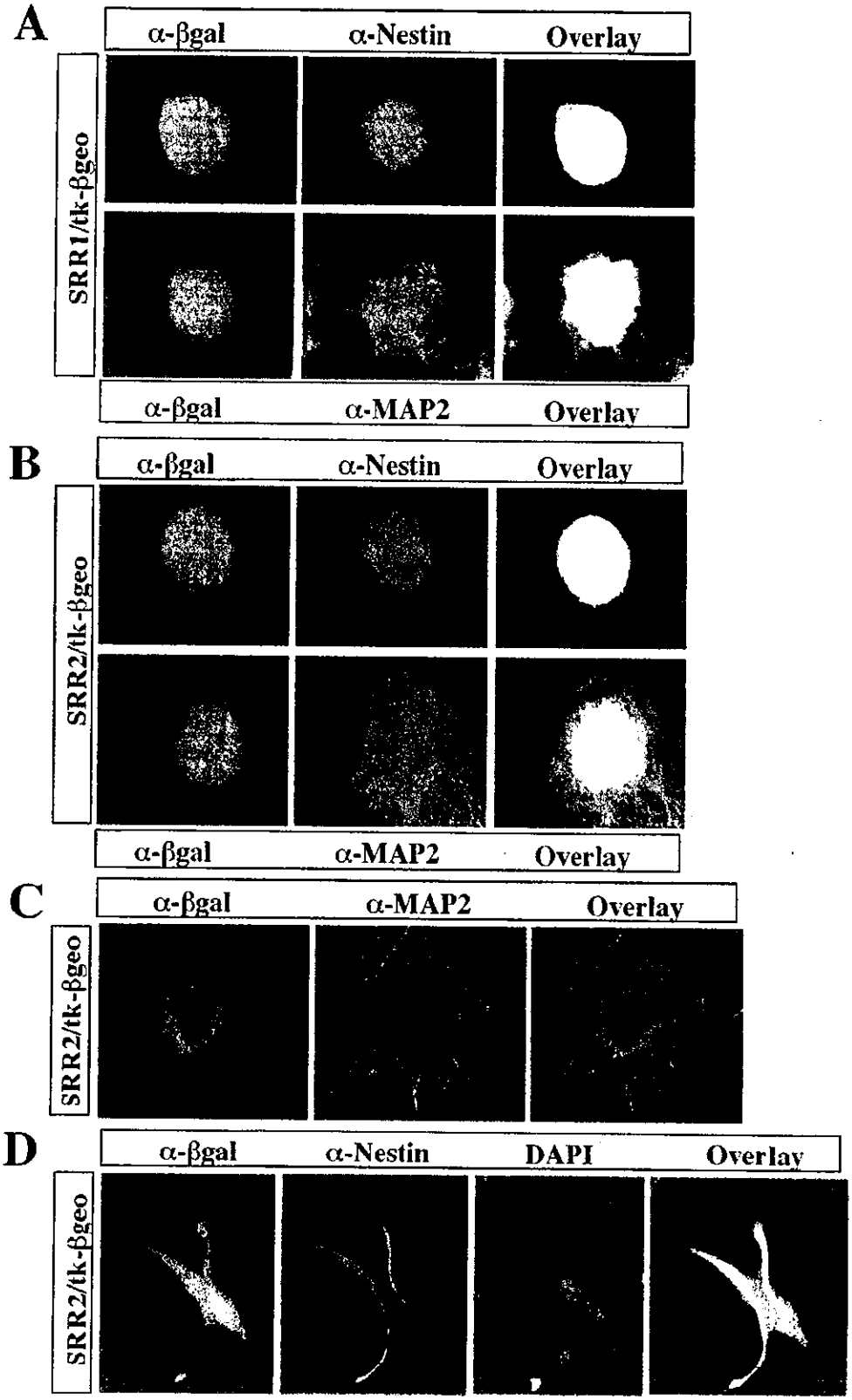

FIG. 2. Function of SRR1 and SRR2 in ES cells subjected to neural differentiation. ES cells carrying SRR1 (A) or the SRR2/tk-β-geo transgene (B) were subjected to neural differentiation using retinoic acid as described by Bain et al. (5). These cells were then cultured on coverslips coated with PDL and laminin for 2 days. After fixation, these cells were immunostained with a combination of two stains, either nestin–β-Gal or MAP2–β-Gal. (C) The ES cells carrying the SRR2/tk-β-geo transgene were subjected to neural differentiation and immunostained with MAP2–β-Gal as described for panel B. These cells were then inspected with a confocal microscope. (D) The ES cell-derived neural cells bearing the SRR2/tk-β geo transgene were dissociated to the single-cell level, transferred to coverslips coated with PDL and laminin, and immunostained with nestin–β-Gal. α, antibody.

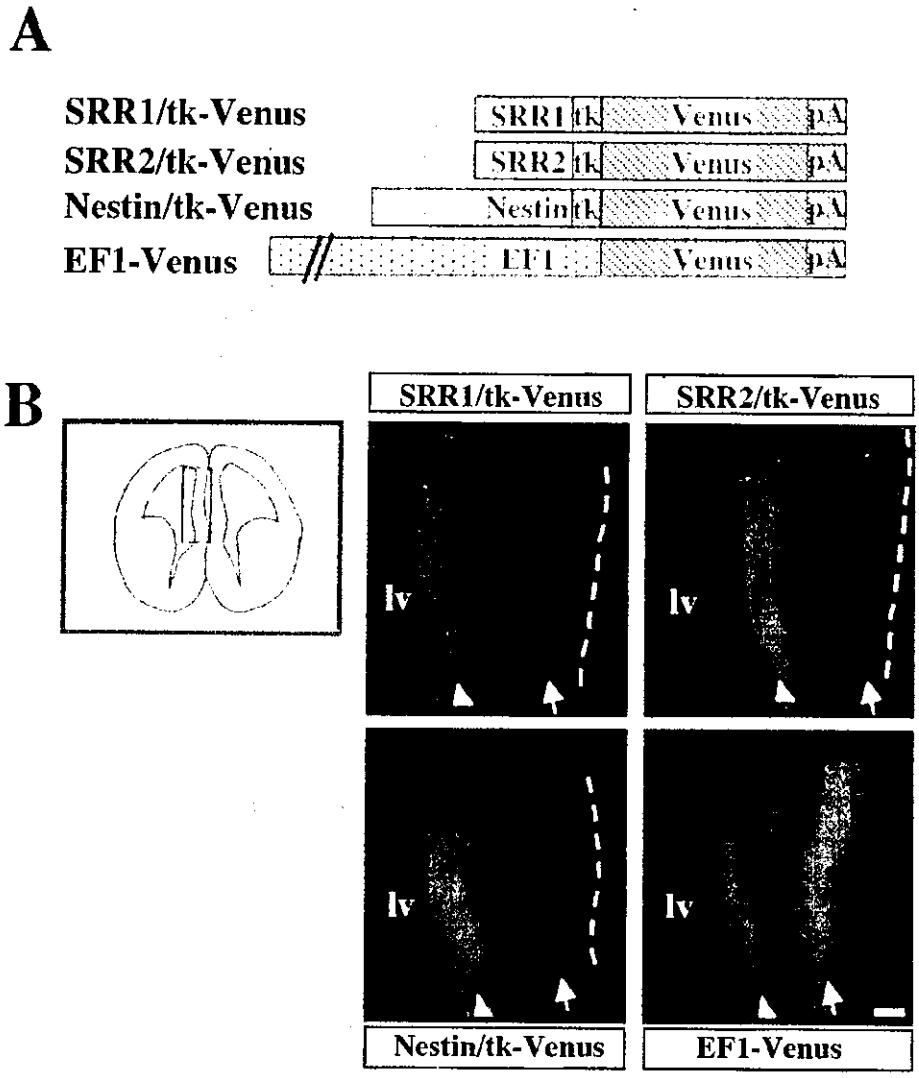

FIG. 3. Characterization of SRR1 and SRR2 activities in the developing brain by in vivo electroporation. (A) Reporter plasmids used for in utero electroporation. pA represents the poly(A) signal from simian virus 40. (B) SRR1 and SRR2 support rather specific reporter gene expression in the ventricular zone of the developing brain. The reporter plasmids were electroporated into E13.5 mouse brain. The red rectangle represents the brain portion in which the reporter plasmids were introduced. After 4 days, brains were recovered from fetuses and sliced with a vibratome, and reporter gene expression was inspected. The dorsal portion is to the top, while the medial portion is to the right. Arrowheads and arrows indicate the ventricular zone and cortical plate of the brain, respectively, while dotted lines correspond to the outer surface of the brain. lv, lateral ventricle. The white bar corresponds to 100 μm.

been shown that the protein is required for the development of trophoblastic stem cell-derived extraembryonic ectodermal tissues (4). Therefore, we examined whether SRR1 and SRR2 can also function in the trophoblast stem cells. To address this issue, we used a genetically manipulated ES cell line, ZHBTc4, in which the *Oct-3/4* gene shows tetracycline-regulated expression. This ES cell line can be easily converted to cells with trophoblast stem cell characteristics by culturing in the presence of FGF-4, heparin, and tetracycline but in the absence of leukemia inhibitory factor (32, 44). The SRR1, SRR2, *UTF1*, and *EF1* regulatory regions were individually connected to the *puro-Venus* reporter gene, which encodes a fusion protein of Venus and puromycin-detoxifying enzyme (see Materials and Methods). Subsequently, these reporter genes were introduced to the ES cells by lipofection, and stable puromycin-resistant transformants were obtained based on these enhancer activities in pluripotent ES cells. The activities of these regulatory regions in the ES cells were evident not only by the puromycin-resistant phenotype but also from the fluorescence of the fusion protein (Fig. 4A). However, when these cells were converted to trophoblast stem cell-like cells, fluorescence from the fusion protein was concomitantly extinguished in all cases except in the cells bearing the EF1-puro-Venus reporter gene. We also examined reporter gene expression by Western blot analysis using an anti-GFP polyclonal antibody which recognizes Venus. Consistent with the data shown in Fig. 4A, none of the regulatory regions except for the *EF1* promoter were able to contribute to the production of a detectable amount of

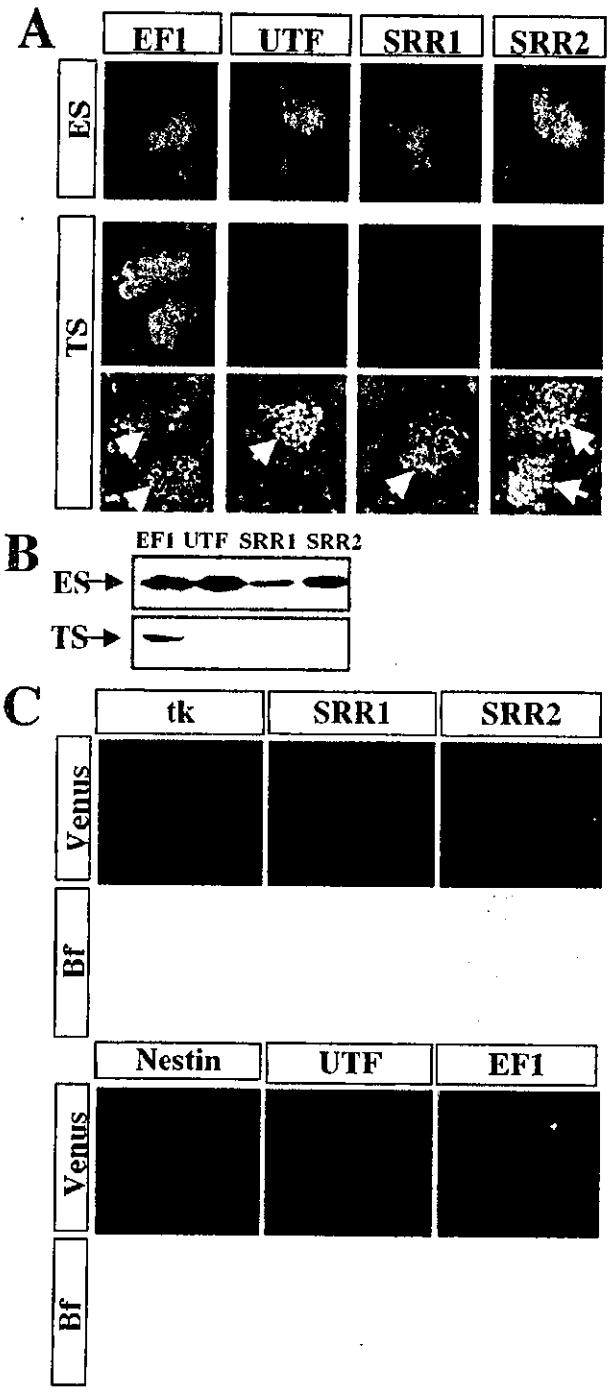

FIG. 4. SRR1 and SRR2 do not function in trophoblast and hematopoietic stem cells. (A) Functional analyses of SRR1 and SRR2 in ES cells and trophoblast stem cell-like cells. The *puro-Venus* reporter genes bearing the indicated regulatory regions were introduced to ZHBTc4 ES cells (32), and puromycin-resistant transformants were obtained. These ES cells were then converted to cells with trophoblast stem cell characteristics as described by Niwa et al. (32). Typical examples of stable ES cell transformants and cells converted to trophoblast stem cell-like cells were shown under fluorescence microscopy. The latter cells were also counterstained with DAPI (4′,6′diamidino-2-phenylindole). Arrows indicate ES cell-derived trophoblast stem cell-like cells with a regular epithelial cell morphology (44). TS, trophoblast stem cell-like cells. (B) Expression level of puro-Venus protein in ES cells and trophoblast stem cell-like cells. Whole-cell extracts were prepared from various ES cells and trophoblast stem cell-like cells, and Western blot analyses were performed using anti-GFP antibody, which recognizes the Venus portion of the fusion protein. (C) SRR1 and SRR2 fail to display their enhancer activities in hematopoietic stem cells. The hematopoietic stem cell-enriched CD34$^-$ KSL cell population from mouse bone marrow was prepared according to the method of Osawa et al. (33) and transduced with the lentiviruses shown in Fig. 1A. After 48 h, the production of Venus reporter protein was inspected.

the fusion protein in these trophoblast stem cell-like cells, although all of these regulatory regions were able to support reporter gene expression in ES cells (Fig. 4B). It should be noted that a high level of endogenous *Sox-2* gene expression is detected in these cells (data not shown). Thus, these results postulate that both SRR1 and SRR2 fail to support gene expression in trophoblast stem cells and that *Sox-2* expression in these cells is supported by a distinct regulatory region(s).

We next examined the possible function of SRR1 and SRR2 in hematopoietic stem cells. Although the *Sox-2* gene appears not to be expressed in hematopoietic stem cells (36), there is the possibility that these isolated regulatory regions somehow function in these cells. For this purpose, we transduced the reporter genes into CD34$^-$ KSL cells, which are a highly enriched cell population for hematopoietic stem cells (33), using the same set of VSV-G pseudotype lentiviruses used to obtain the results shown in Fig. 1. Only the *EF1* promoter exerted its activity in these hematopoietic cells, whereas all of other regulatory regions did not show a detectable effect on the expression of the reporter gene in these cells (Fig. 4C). Thus, together with the fact that both SRR1 and SRR2 fail to function in trophoblast stem cells, these regulatory regions do not promiscuously show their transcription-stimulating activities in stem cells.

Immunohistochemical analyses of cells in which SRR2 functions in the developing brain. For subsequent analyses, we decided to concentrate on SRR2 in the developing brain because we have already systematically analyzed the molecular basis of SRR2 activity in ES cells (48). That is, we believe that similar systematic analyses of the region in neural stem and progenitor cells may allow us to compare for ES and neural stem cells the molecular bases of SRR2-mediated transcriptional stimulating activity.

Based on these considerations, we first examined molecular aspects of the cells in which SRR2 functions in the developing brain. After electroporation with the SRR2/tk-Venus reporter plasmid, brain slices were immunostained for Venus protein together with antibody for nestin or MAP2 protein. We also examined the endogenous Sox-2 protein by the same procedure. As shown in Fig. 5A, endogenous Sox-2 was present rather predominantly in the ventricular zone of the 17.5-d.p.c. embryonic brain. Similarly, SRR2 directed Venus reporter expression rather specifically in the ventricular zone (Fig. 5B). Anti-nestin antibody revealed that the expression of Venus and the expression of nestin overlapped in the ventricular zone (Fig. 5B to D; magnified views are shown in panels E to G). To determine this coexpression conclusively, cells were recovered from developing brains after electroporation of the reporter

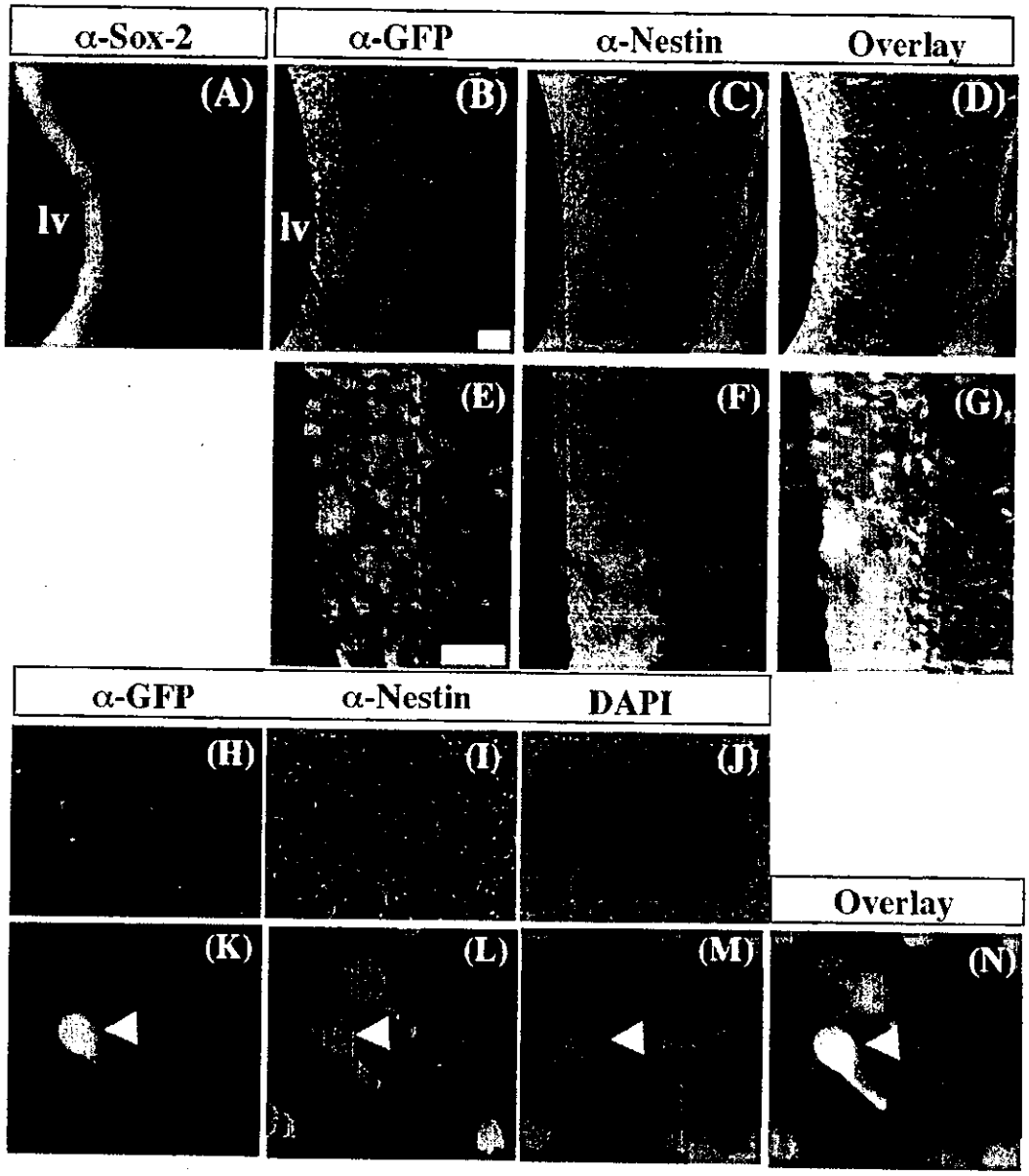

FIG. 5. SRR2 exerts its enhancer activity in neural stem or progenitor cells but not in postmitotic neurons in developing brains. Sections from normal E17.5 mouse brain (A) or brains in which the SRR2/tk-Venus reporter gene had been introduced by in vivo electroporation (B to G and O to T) were immunostained. (H to N) Cells were recovered from brains after incorporation of the reporter plasmid by in utero electroporation, transferred to a coverslip, and immunostained. The antibodies (α) used are indicated at the top of each panel. (E to G) Magnified views of panels B to D. The orientation of the brain sections is the same as that shown in Fig. 3B. White bars in panels B, E, O, and R correspond to 100 μm. Arrows in panel T indicate cells which are doubly positive for GFP and phosphorylated histone H3. lv, lateral ventricle.

plasmid. These cells were then transferred to coverslips and immunostained for Venus and nestin. Representative data are shown in Fig. 5H to N. These analyses revealed that about 92% of Venus-positive cells were nestin positive. We assume that cells which were positive for nestin but negative for Venus in most cases represent cells that were not transfected with the reporter gene. We also compared the levels of expression of Venus and MAP2 and found that the expressions of these proteins were mutually exclusive (Fig. 5O to Q). Analyses of the expression of Venus and phosphohistone H3, a specific marker for mitotic cells revealed that some of the Venus-positive cells were also positive for phosphohistone H3 (Fig. 5R to T). Again, cells which were positive for phosphohistone H3 but negative for Venus were assumed to be nontransfected cells. In any event, from these results, we conclude that, as in in vitro-cultured cells, SRR2 exerts its function mainly in rapidly proliferating nestin-positive neural stem or progenitor cells and not in MAP2-positive postmitotic neurons in the developing brain.

From the homogeneous expression profile of the *Venus* re-

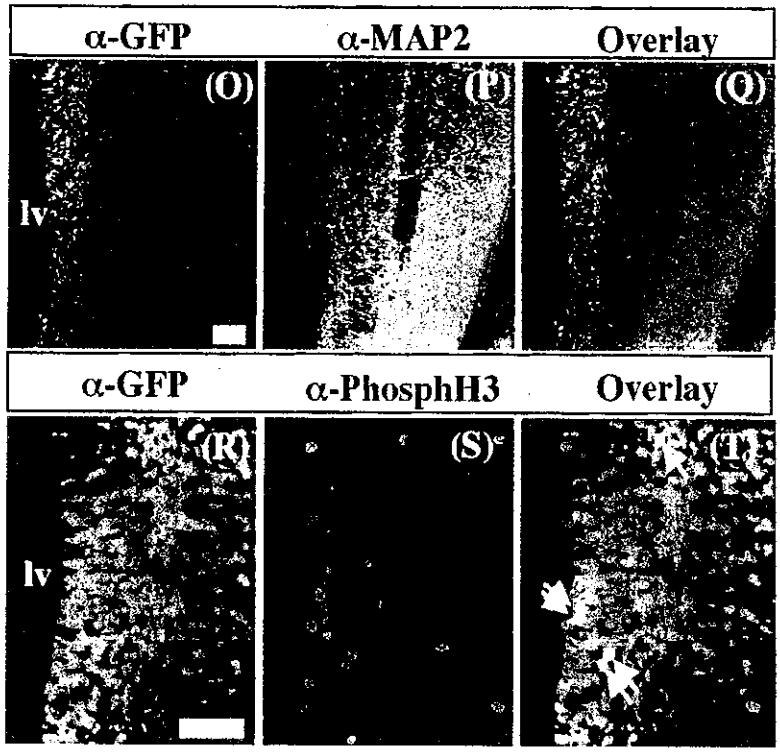

FIG. 5—*Continued*

porter gene in the ventricular zone of the embryonic brain, it is obvious that SRR2 exerts its activity in neural progenitor cells. However, none of the above-described analyses unequivocally demonstrate that SRR2 functions in multipotent neural stem cells. Thus, we performed a clonogenic analysis to examine whether SRR2 is also active in neural stem cells. By this method, neurospheres were generated from fetal brains in which the SRR2/tk-Venus reporter gene had been introduced by in vivo electroporation and plated at clonal density. Then, a spherical colony generated from a single Venus-positive cell shown in Fig. 6A was recovered. By following the same protocol, we also prepared neurospheres from healthy developing brains in which no DNA had been introduced and compared the self-renewal activities of neurospheres derived from non-selected control cells and those derived from a single cell in which SRR2 functioned. As shown in Fig. 6B, these analyses revealed that the cells in which SRR2 functioned showed activity comparable to that of control neurosphere cells in terms of their ability to produce secondary neurospheres. We next examined multipotent properties of the cell in which SRR2 functioned. After trypsinization and expansion of neurospheres derived from a single Venus-positive cell, immunostaining analyses were performed after induction of differentiation with FBS. As shown in Fig. 6C to E, these cells generated both MAP2-positive neurons and GFAP-positive astrocytes upon differentiation. Figure 6F to H show that neurosphere cells derived from the same single cell generated O4-positive oligodendrocytes as well as GFAP-positive astrocytes. Thus, these results confirmed that the cells in which SRR2 functioned gave rise to all three different neural lineages when cells were induced to differentiate. From these results, we conclude that at least a portion of cells showing SRR2-dependent Venus expression in the developing brain are multipotent neural stem cells.

The same core sequence of SRR2 is involved in gene expression in ES cells and neural stem or progenitor cells. To localize the SRR2 core sequence involved in gene expression in neural stem or progenitor cells, we made a series of internal-deletion mutants of SRR2 connected to the *Venus* reporter gene (Fig. 7A). Subsequently, these plasmids were individually introduced into the 13.5-d.p.c. mouse brains by in utero electroporation. After 48 h, brains were recovered and Venus expression was examined as described for Fig. 3B. These analyses revealed that the transcription-stimulating activity of SRR2 was profoundly impaired in the del.9 and del.10 mutants but that all of the other mutants showed activities equivalent to that of wild-type SRR2 (Fig. 7B). It should be noted that deleted regions of these mutants encompass the octamer and Sox-2 binding site-like sequences which have been shown to play a critical role in the enhancer activity of SRR2 in ES cells (48). To examine the possible involvement of the octamer and Sox-2 binding site-like sequences in SRR2 in the neural stem or progenitor cell population, we made two different nucleotide substitution mutants, mutOct and mutSox, in which octamer and Sox-2 site-like sequences were impaired so as not to serve as octamer factor and Sox binding sites, respectively (see Materials and Methods). The transcription-stimulating activities of these SRR2 mutants were analyzed in developing brains as described above. These analyses revealed that both of these mutants failed to exhibit significant activities in this system,

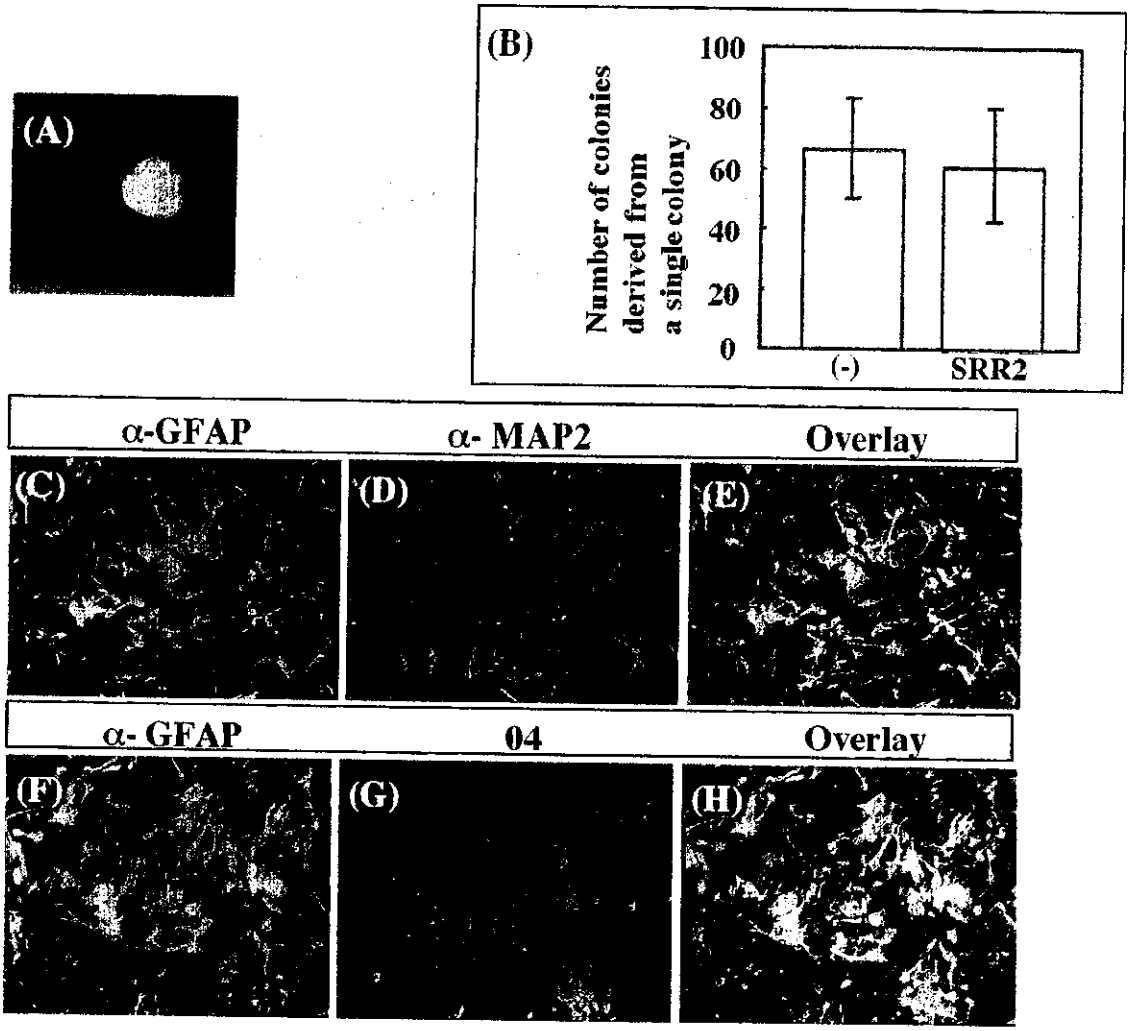

FIG. 6. Cells in which SRR2 functions were converted to all three different neural lineages (neuron, astrocyte, and oligodendrocyte) upon differentiation. (A) Preparation of neurospheres generated from a single cell in which SRR2 functions. Neurospheres prepared from SRR2/tk-Venus-transfected brains were plated at clonal density with serum-free medium containing basic fibroblast growth factor and epidermal growth factor for 7 days, and neurospheres derived from single Venus-positive cells were selected. (B) Self-renewal activity of cells in which SRR2 functions. Neurospheres of similar size (about 0.2 mm in diameter) derived from a single Venus-positive cell were individually dissociated and recultured. The number of generated colonies was counted under a microscope. The data were obtained from 16 independent colonies. The neurospheres derived from nontransfected brain were used as a control. (C to H) Multipotent properties of cells in which SRR2 functions. The expanded neurospheres derived from a single cell in which SRR2 functions were dissociated, split into two wells of a slide chamber coated with PDL and laminin, and cultured in medium containing 1% FBS. After 7 days, cells were fixed and subjected to immunostaining procedures. One of the chambers was stained with anti-GFAP and anti-MAP2 antibodies (C to E), while the other was stained with anti-GFAP antibody and O4 antibody (F to H). Venus protein is not present in the differentiation-induced cells at a detectable level (data not shown), and the green fluorescent color in panels C and F is exclusively due to Alexa Fluor 488 dye-conjugated secondary antibody bound to cells via the GFAP–anti-GFAP antibody complex. α, antibody.

indicating that, as in the ES cells, both the octamer and Sox-2 binding site-like sequences play a pivotal role in supporting the enhancer activities of SRR2 in developing brains. Moreover, these octamer and Sox-2 binding site-like sequences, when multimerized to four copies, were sufficient to support ventricular-zone-restricted reporter gene expression in developing brains.

We have previously demonstrated that the Oct-3/4–Sox-2 complex makes a major contribution to SRR2 activity in ES cells (48). Because the same or at least overlapping regulatory sequences are involved in SRR2 activity in neural stem or progenitor cells, it is possible to assume that a similar protein complex(es) supports SRR2 activity in the brain. However, Oct-3/4 protein is not present in the brain, although Sox-2 is present in neural stem or progenitor cells. Therefore, it is conceivable that certain other octamer factors present in the developing brain may contribute to SRR2 activities in this tissue. We note from the literature (1, 9, 13, 16, 23, 41, 42) and microarray analyses (N. Masuyama, S. Miyagi, A. Okuda, and Y. Gotoh, unpublished data) that four different octamer fac-

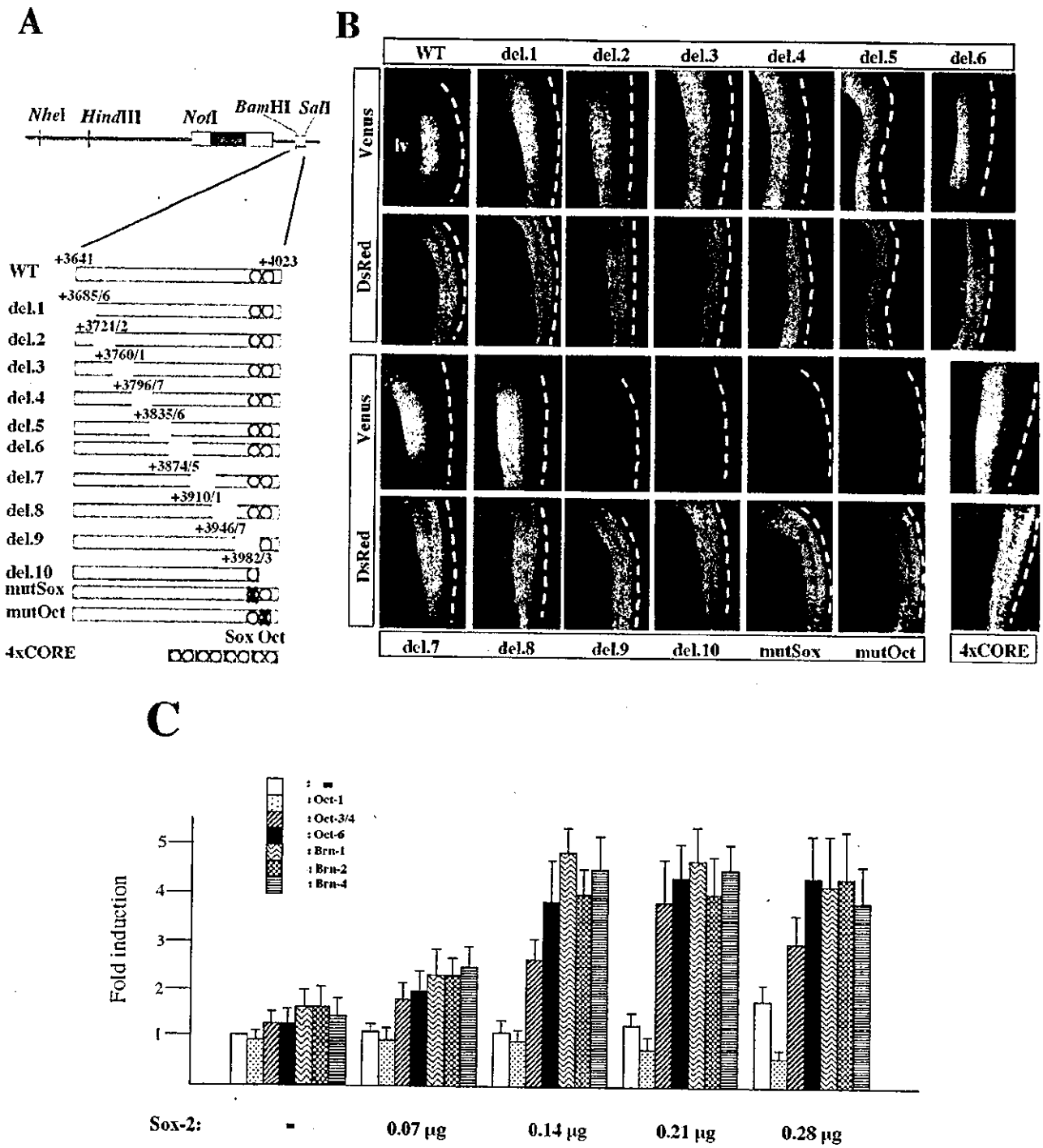

FIG. 7. The same core sequence of SRR2 is involved in its enhancer activities in ES cells and neural stem or progenitor cells. (A) Schematic representation of wild-type (WT) and various types of mutants of SRR2. "del." followed by a number indicates a mutant regulatory region with a deletion. The Sox- and Oct-like sequences are indicated as filled and open circles, respectively. The open and filled boxes represent noncoding and coding regions of the *Sox-2* gene, respectively. Numbers represent the positions where the adenine nucleotide of the transcription initiation codon is set to +1. These DNA fragments were subcloned into the pik-Venus reporter plasmid. (B) The *Oct-* and *Sox*-like elements of SRR2 are required for its enhancer activity in neural stem cells. The *Venus* reporter plasmids shown in panel A were introduced into E13.5 mouse brain together with an internal control *DsRed* reporter gene, which is connected to the chicken β-*actin* promoter. After 48 h, *Venus* and *DsRed* reporter gene expression was inspected. The orientation of sectioned brains was the same as that in Fig. 3B. (C) All of the POU III class octamer factors expressed in brain show the potential to augment SRR2 activity together with Sox-2. COS cells were transfected with 0.07 μg of octamer factor expression vectors and with increasing amounts of Sox-2 vector, as indicated, as well as ik-Luc reporter plasmid (0.7 μg) bearing SRR2. An internal control luciferase gene (0.7 μg) of *Renilla reniformis* were also transfected. The transcriptional level was estimated as described in Materials and Methods. Data were obtained from five independent experiments with comparable results.